EXPERIMENTAL STRATEGY FOR THE DETERMINATION OF HEAT TRANSFER COEFFICIENTS IN PEBBLE-BEDS COOLED BY FLUORIDE SALTS

L. Huddar, P. F. Peterson
Department of Nuclear Engineering, University of California, Berkeley, CA 94720, USA
lakshana.huddar@berkeley.edu, peterson@nuc.berkeley.edu

R. Scarlat
931 Engineering Research Building, Madison, WI 53711, USA
Department of Engineering Physics, University of Wisconsin Madison
roscarlat@wisc.edu

Z. Guo
Department of Nuclear Engineering, University of California, Berkeley, CA 94720, USA
Department of Nuclear Science and Technology, Xi'an Jiaotong University, Xi'an, 710049, China
zhangpengguo@berkeley.edu

ABSTRACT

It is important to accurately model the heat transfer coefficient between the fuel pebbles and the flibe coolant in order to correctly predict fuel temperatures in the core of the fluoride-salt-cooled, high temperature reactor (PB-FHR). We have been performing experiments using simulant oils that match key non-dimensional parameters expected in PB-FHRs. A 3.5" long test section is filled with ¼" copper pebbles, some of which are instrumented with thermocouples. Oil is circulated through the test section. The entering temperature of the oil is varied, and the time-varying exit temperature of the oil and temperatures of the instrumented pebbles are recorded. Using these temperatures the interfacial heat transfer coefficient can be extracted as a function of position and time. Correlations for interfacial heat transfer coefficients are available in the literature, but these are derived using experimental data that do not entirely encompass PB-FHR operating conditions. Generally for the PB-FHR the Reynolds and Prandtl numbers during normal operation are higher than reported experimental results. Thus, it is important to perform tests in the appropriate PB-FHR Reynolds and Prandtl number range. Preliminary results indicate that experimentally measured heat transfer coefficients may be at least 20% higher than predicted using Wakao and Funazkiri's correlation for Nusselt number in pebble beds. These preliminary results also reinforce the need to reduce uncertainties in the collected data. This paper will also present experimental techniques that aim to accomplish this. Specifically, we detail how frequency response techniques can be used to extract heat transfer coefficients from a pebble-bed test section and how experiments can be designed using simulant oils to achieve this.

KEYWORDS
FHR, pebble-bed, heat transfer coefficient, simulant oils, scaled experiments.

1. INTRODUCTION AND BACKGROUND

Fluoride-salt-cooled high temperature reactors (FHR) make up a class of advanced nuclear reactor designs. The University of California, Berkeley, is investigating a small modular pebble-bed reactor (PB-FHR). One of the key phenomena of interest is the high Prandtl number coolant heat transfer in the pebble bed core. The core is composed of spherical fuel elements that are randomly packed in an annular cylindrical geometry. The heat transfer coefficient between the pebbles and the coolant needs to be well characterized in order to be able to predict the fuel and flibe temperatures in the reactor. Additionally, the heat transfer coefficient needs to be known for a range of Reynolds numbers. We use simulant oils in place of flibe, the PB-FHR main coolant, while matching Prandtl and Reynolds numbers between the experiment and the prototypical system [1].

1.1 Literature Review

Wakao's review paper lists all the experimental data that was collected for heat transfer coefficients in packed beds as a function of Reynolds and Prandtl numbers [2]. The majority of the data was collected for air or water. The range of Reynolds for their proposed correlation was from 15-8500. The experimental data that this correlation was based on were all done with air or other gases, with Prandtl numbers ranging from 0.7 to 1. The correlation proposed by Wakao and Funazkri is widely used in packed bed heat transfer predictions. Carillo finds the heat transfer coefficient between oil and a bed of steel spheres, and also studied the effect of porosity on the Nusselt number. They propose correlations for five different porosities for ranges of Reynolds numbers that go from 0.53 up to 412 [3]. Geb et al. flow air through a randomly packed test section of steel pebbles heated via induction for a range of Reynolds numbers from 20 to 500 [4]. This was done for a non-infinite bed so wall effects played a role in the lower than expected measured Nusselt numbers. Handley and Heggs develop a correlation for heat transfer in fixed packed beds for Reynolds numbers higher than 100 [5]. In the current work, heat transfer coefficient is measured for higher Prandtl numbers, in the range important for heat transfer to molten salts, and a range of Reynolds numbers in an 'infinite' randomly packed pebble bed using oil as the heat transfer fluid.

1.2 Experimental Aims of the Current Investigation

There were three main aims to the experiment:

(1) To measure heat transfer coefficients in pebble beds for a range of Reynolds and Prandtl numbers applicable to the pebble-bed FHR (PB-FHR) cores, and understand any reasons for potential discrepancies between measured values and values predicted using correlations from the literature
(2) To develop an experimental basis for heat transfer coefficients in pebble beds for a range of Reynolds and Prandtl numbers beyond those expected for FHRs during normal operation
(3) To generate data that could be used to confirm the use of simulant oils in predicting the heat transfer behavior in pebble beds cooled by fluoride salts.

1.3 Structure of the Paper

The experimental procedure using a step change in the inlet fluid temperature is first outlined. This includes the design of pebble bed test section and the use of simulant oils. The data reduction procedure is shown and the sources of potential errors are discussed. The results obtained from these experiments are shown. Since all the aims outlined in Section 1.2 were not achieved in this first set of experiments, the design for another experimental facility is described. This new experimental facility design is optimized to measure heat transfer coefficients in the pebble bed test section using frequency response techniques. The paper ends with conclusions drawn from the first experimental effort and provides recommendations for how experimental data can be best collected going forward.

2. EXPERIMENTAL PROCEDURE

An experimental loop was constructed for the purpose of measuring heat transfer coefficients in a pebble-bed test section. A test section was filled with randomly packed copper pebbles, and was heated to an initial temperature. Then cold fluid was passed through the test section and the temperatures of the pebbles and the fluid inlet and outlet temperatures were recorded throughout the thermal transient using Type T Omega manufactured thermocouples embedded inside selected pebbles. These temperatures were then used to extract the heat transfer coefficient between the pebbles and the surrounding fluid as a function of time and axial location. The mass flow rate throughout the transient was also recorded using a Coriolis flow meter (Siemens MASSFLO MASS 2100 DI). The experimental facility is shown in Figure 1.

2.1 Test Section Design

The test section is cylindrical, with a length of 88.9 mm (3.5 inches) and a diameter of 44.5 mm (1.75 inches) and is filled with 0.00635 mm (1/4 inch) diameter copper pebbles. The wall of the test section is dimpled to break up ordered packing of the pebbles at the wall in order to better simulate an infinite bed. A picture of the test section is shown in Figure 2. Some of these pebbles were instrumented with thermocouples. Thermocouples were also used to measure the bulk fluid temperature at the inlet and outlet of the test section. Figure 3 shows the location of thermocouples within the test section. Pebble temperatures in various axial and radial locations in the test section were recorded. The instrumented pebbles had holes drilled to their centers where thermocouples were cemented. Because of the high thermal conductivity of copper, the pebble surface temperature can be assumed to be the same as the center temperature. The Biot number ranges in an individual copper sphere was from 0.005 to 0.024, which is smaller than 1. Thus, this approximation is justified.

Figure 1: Test section filled with copper pebbles for heat transfer coefficient measurement experiments

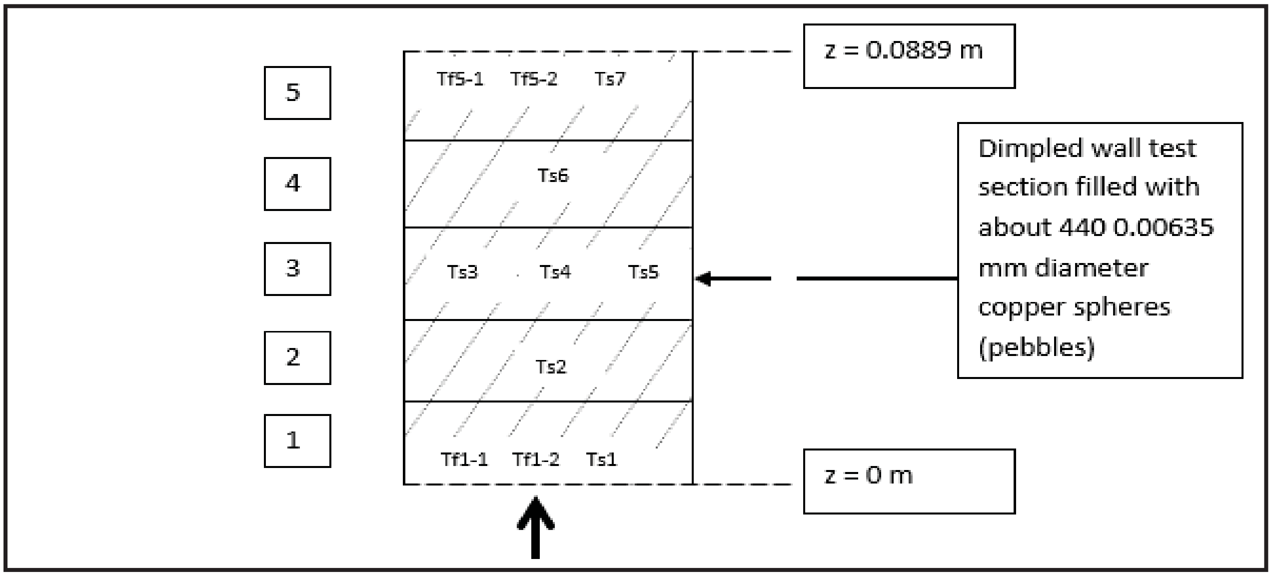

Figure 2: The test section is divided into 5 axial regions. Instrumentation locations for pebbles (labelled with ‘s’) and bulk fluid temperatures (labelled with ‘f’) are shown.

2.2 Use of Simulant Oils as the Heat Transfer Fluid

We use Dowtherm A and Drakesol 260AT to simulate the molten salt flibe, which would be used to cool pebble bed FHRs. Table 1 shows typical Reynolds and Prandtl numbers in a PB-FHR core during normal operation (forced circulation) [6] and Table 2 shows the obtainable ranges of non-dimensional numbers using the simulant oils. Currently, experiments have been carried out using Drakesol 260AT only. The lowest achievable Prandtl number of the Drakesol 260AT is still higher than for Dowtherm A because of the higher viscosity. Since experimental data in this range is generally lacking, it is helpful to collect this data even if the Prandtl range does not overlap with the PB-FHR operating conditions. The physics of the heat and momentum transfer at Prandtl numbers higher than unity is very different to Prandtl numbers smaller than unity, so any data collected at higher Prandtl numbers is still valuable. Reynolds and Prandtl numbers are defined in Equations (1) and (2).

$$Reynolds = \frac{Superficial\ velocity \times pebble\ diameter}{fluid\ kinematic\ viscosity} \qquad \mathrm{Re} = \frac{Ud}{\nu} \tag{1}$$

$$Prandtl = \frac{fluid\ momentum\ diffusivity}{fluid\ thermal\ diffusivity} \qquad \mathrm{Pr} = \frac{\nu}{\alpha} \tag{2}$$

The superficial velocity U is defined as the velocity through an empty pebble-bed in m/s, the diameter d refers to the pebble diameter in m, and the fluid properties ν and α refer to the kinematic viscosity (in units of m^2/s) and thermal diffusivity (in units of m^2/s) taken at film temperatures, which is defined in Section 5.2 in Equation (5). Drakesol 260AT matches the Prandtl number of flibe at temperatures between 60°C and 140°C as shown in Figure 4.

Table 1 shows the Reynolds and Prandtl number ranges for the 236 MWth PB-FHR design during normal operation, which corresponds to forced circulation through the pebble bed core, and emergency shutdown cooling, which corresponds to natural circulation through the reactor core. These are approximate based on the average inlet and outlet temperature in the reactor core, 600 °C and 700 °C respectively. We attempted to achieve the correct range of Reynolds and Prandtl numbers in the experiment.

Table 1: Typical non-dimensional parameter values in the PB-FHR reactor core for forced circulation (power operation) and natural circulation (decay heat removal)

	Reynolds in the core	Prandtl in the core
Forced circulation	900-1000	20-10
Natural circulation	10-20	20-10

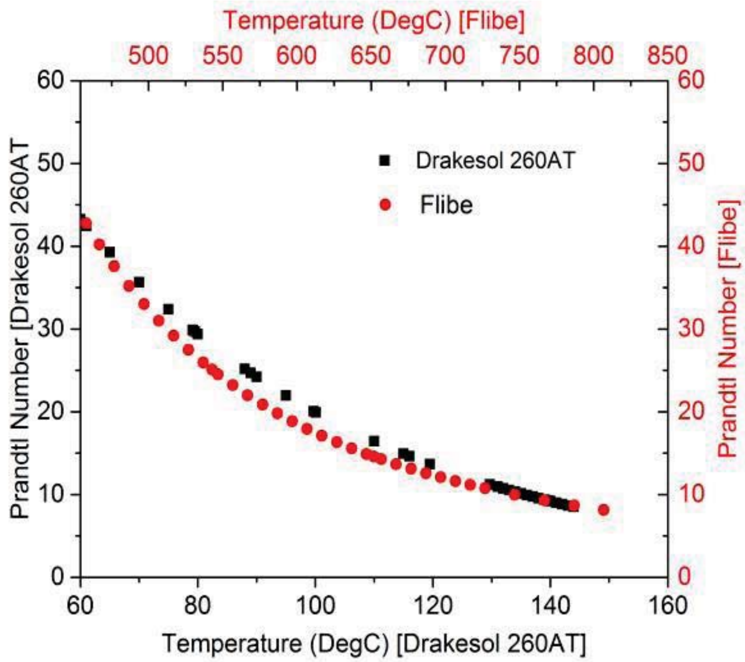

Figure 3: Prandtl number comparison of the simulant oil Drakesol 260AT and Flibe

The procedure for heating the oil to the required temperature is outlined in Figure 5. In Phase I, flow is directed simultaneously through the test section branch and the heater branch. Thus the test section temperature can be increased to the desired value. The maximum oil temperature that was obtained with the Drakesol 260AT was 60 °C. In Phase II, the oil was rapidly cooled down using the bypass branch, at which time the other two branches were valved off. During this phase the loop was actively cooled by running chilled water through the heat exchanger. It is important to note that the test section had insulation wrapped around it. Thus the temperature of the test section was maintained throughout the entirety of Phase II. The duration of Phase II is ~15 seconds. The aim of this phase is to decrease the oil temperature by a minimum of 5 °C, so the temperature difference between the pebbles and the fluid will be sufficiently large to perform the data reduction with. In Phase III the colder fluid is then re-routed through the test section branch, and then transient data collection begins.

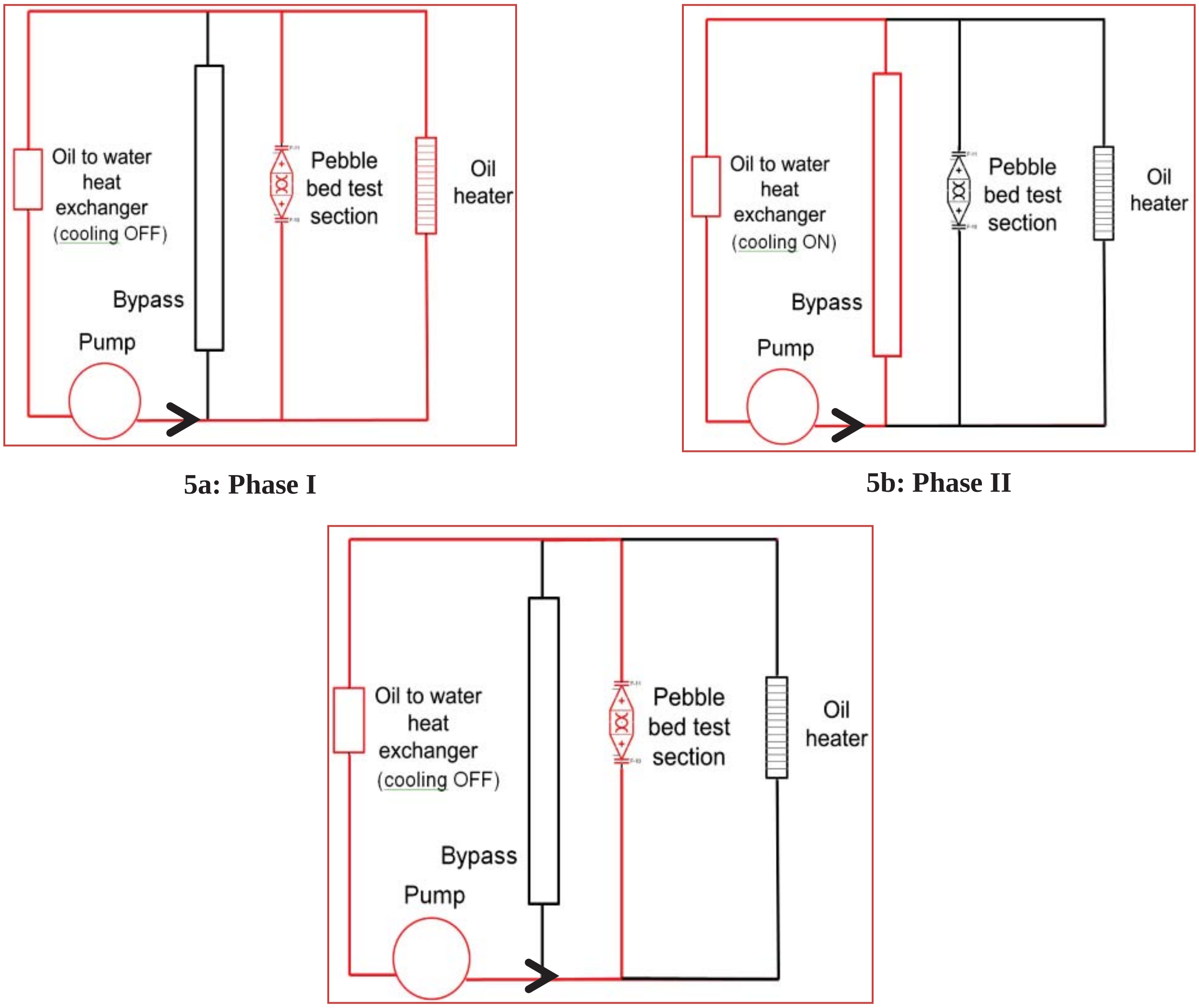

5a: Phase I **5b: Phase II**

5c: Phase III

Figure 4: Procedure for transient heat transfer data collection for the pebble-bed test section divided into three phases. In all schematics, the pump was run in the counter-clockwise direction.

A summary of the experimental runs is given in Table 2. The 'initial ΔT' reported is the temperature difference that was achieved between the entrance control volume section in the test section and the initial inlet fluid temperature as recorded by the thermocouples. 'Transient duration' refers to the time it takes from when the initial cold fluid enters the test section to when the test section reaches equilibrium conditions. This number is much smaller than the fluid residence time in the loop, which implies that the fluid inlet temperature is not affected during the transient.

Table 2: Experimental parameters for the 4 experimental runs

Experimental run	**Reynolds range**	**Prandtl range**	**Initial Δ T in section 1 (°C)**	**Transient duration (s)**
1	322-530	54-55	5.5	1.25
2	26-135	48-58	4	1.5
3	60-175	56-63	4	3
4	79-149	44-53	4	3

3. DATA REDUCTION PROCEDURE

This section covers how the interfacial heat transfer coefficient was determined from the raw experimental data and when parameters went into the uncertainty analysis procedure. There is also a discussion about the assuming quasi-steady state conditions during the experiment.

3.1 Deriving Experimental Interfacial Heat Transfer Coefficient

The heat transfer coefficient is extracted from the temperature data by equating the rate of change of internal energy of the pebbles and the convective heat transfer between the pebbles and the surrounding fluid, as shown in Equation (3b). Fluid temperatures from the middle sections were estimated using the fluid energy conservation equation using finite differences, as shown in Equation (4). Equation (3b) and (4) can then be used for each control volume section. Thus the heat transfer coefficient extracted from the data is a function of axial position and time. There is not much variation of temperature in the radial direction in the test section. The variation that is present falls within the error in reading of the Type T thermocouples from Omega Engineering, which is 1°C.

It was found that during equilibrium conditions, the pebble and the fluid thermocouples were not reading the same temperature. This implied that the calibrations of the thermocouples were not as expected. The fluid temperatures generally read lower than the pebble temperatures by about 2.5 degrees at temperatures higher than 50 °C. This was taken into account during the data reduction procedure, by subtracting this discrepancy from the measured difference between pebble and fluid temperature. The uncertainty on the thermocouple readings was a contributing factor to the decision to build a new experimental facility focused on measuring heat transfer coefficients in pebble-beds.

$$(1-\varepsilon)(\rho c_p)_s\left(\frac{\partial T_s}{\partial t}\right)_{section1} = h^*(t)a_v(T_f - T_s(t))_{section1} \tag{3a}$$

$$h^*(t) = \frac{(1-\varepsilon)(\rho c_p)_s\left(\frac{\partial T_s}{\partial t}\right)_{section1}}{a_v(T_f - T_s(t))_{section1}} \tag{3b}$$

$$\begin{aligned}\varepsilon(\rho c_p)_f\left(\frac{\partial T_{f1}}{\partial t}\right)_{section1} + \varepsilon(\rho c_p)_f\left(v_z\frac{\partial T_f}{\partial z}\right)_{section1to section2} &= h_{sf}(T_{s1}-T_{f1})_{section1}\\ \varepsilon(\rho c_p)_f\left(\frac{\partial T_{f1}}{\partial t}\right)_{section1} + \varepsilon(\rho c_p)_f\left(v_z\frac{\Delta T_f}{\Delta z}\right)_{section1to section2} &= h_{sf}(T_{s1}-T_{f1})_{section1}\end{aligned} \tag{4}$$

The definitions of the terms in Equations (3) and (4) are as follows: ε is the porosity, $(\rho c_p)_s$ the volumetric heat capacity of the pebble (copper in the test section), T_s the temperature of the pebble ('solid' phase), t time, h^* the heat transfer coefficient, a_v the specific surface area of the test section, defined in Equation

(10), T_f the oil temperature ('fluid' phase), $(\rho c_p)_f$ the volumetric heat capacity of the oil, v_z the axial superficial velocity of the fluid in the test section, z the axial position co-ordinate and h_{sf} the product of h^* and a_v. The subscript *section 1* refers to control volume section 1, shown in Figure 3. The subscript *1* refers to properties in control volume section 1. The subscript *section 1 to section 2* refers specifically to the advection term, and refers to the axial distance between the entrance to section 1 and the entrance to section 2.

The porosity ε was assumed to be a constant and taken as 0.4 for a loosely-packed randomly packed pebble bed (ref). The porosity will be measured in the next iteration of this experiment. The Nusselt number was predicted at every time step using the measured temperatures to evaluate the relevant non-dimensional numbers. The correlations for Nusselt number along with the definitions for Reynolds and Prandtl are given in Equations (6) and (7). The correlations are referred to as Handley Heggs and Wakao [2], [5] respectively. The KTA correlation [7] was developed for gas cooled pebble-bed reactors and was considered, but was not expected to accurately depict the interfacial heat transfer coefficient of the test section. This is because the Prandtl number range for helium, the coolant of the gas cooled reactors, is about 1, much lower than flibe at the PB-FHR operating temperature which is about 14. The film temperatures were used to evaluate the Reynolds and Prandtl numbers, which were in turn used to evaluate the Nusselt number. The experimental h^* was used to find the experimental Nu_{sf} so it could be compared to the correlations. This was done using Equation (9), which takes into account the particle conductivity [8]. The film temperature is defined in Equation (5). The film temperature is used because it is the average temperature across the thermal boundary layer over each pebble.

$$T_{film} = \frac{T_s + T_f}{2} \tag{5}$$

$$Nu_{sf} = \frac{0.255}{\quad} \Pr^{1/3} \mathrm{Re}^{2/3} \tag{6}$$

$$Nu_{sf} = 2 + 1.1 \Pr^{1/3} \mathrm{Re}^{0.6} \tag{7}$$

$$h_{sf} = a_v h^* \tag{8}$$

$$\frac{1}{h^*} = \frac{d}{Nu_{sf} k_f} + \frac{d}{k_s} \tag{9}$$

$$a_v = \frac{6(1 \quad)}{d} \quad \text{so} \quad a_v = \frac{6(1 \quad 0.4)}{0.00635} = 567 m^{\ \ 1} \ \text{in the test section} \tag{10}$$

k_f is the thermal conductivity of the oil in $Wm^{-2}K^{-1}$, k_s is the thermal conductivity of the copper in $Wm^{-2}K^{-1}$, Pr the Prandtl number (as defined in Equation (2)), Re the Reynolds number (as defined in Equation (1), d the particle diameter in m, β a geometrical constant depending on the shape of the particle (for spheres it is 10).

In the current study the heat transfer coefficients from the central three sections (sections 2, 3 and 4 in Figure 3) have not been evaluated given the uncertainties in the thermocouple readings of the fluid bulk temperatures. These are the temperatures that would be used to estimate the fluid temperature within the test section. The next iteration of this experiment aims to ensure that heat transfer coefficients from the central control volume sections can be measured with reasonable accuracy.

3.2 The Assumption of Quasi-Steady State Conditions

Although this experiment is a transient study, quasi-steady state conditions can perhaps be assumed. The ratio of the volumetric heat capacity between the fluid and solid phases is an indicator for whether quasi-steady conditions may be assumed. Figure 6 shows the volumetric heat capacities of the copper pebbles and the Drakesol 260AT oil. If the ratio of $(\rho c_p)_f / (\rho c_p)_s$ is smaller than 1, this implies that the temperature of the solid changes more slowly than the fluid temperature. This is the case with the Drakesol 260AT oil and copper, with a ratio of 0.44. This ratio is smaller than 1 but still close to unity. This means that there may be distortions due to transient effects. The measured heat transfer coefficients are being compared to steady state correlations. The new experiment discussed in Section 5 of this paper should be able to reduce any distortions due to transient effects as the temperature differences are designed to be periodic.

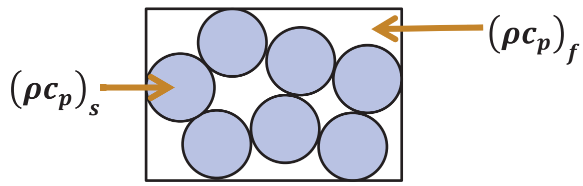

Figure 5: Diagram of pebbles and oil (solid and fluid phases)

3.3 Uncertainty Analysis Procedure

The biggest contributions to uncertainty in the experimentally derived h^* are from dT_s/dt, T_s and T_f. The porosity ε also has an associated uncertainty with it since it was not measured prior to the tests. It is important to note that the uncertainty analysis is approximate because the uncertainties associated with the material properties of the operating fluid Drakesol 260AT are unknown. The thermal conductivity and specific heat capacity of Drakesol 260AT were assumed to be constants, which may not be the case because these properties are temperature dependent in other similar oils. It was assumed that the uncertainty in the Drakesol 260AT properties were about 10%. The uncertainties associated with the properties of copper were assumed to be small enough to neglect. Uncertainty is also associated with the predicted Nusselt numbers, as the non-dimensional numbers used to calculate them were based on fluid temperatures. Thermocouple errors are associated with them. Table 3 shows the uncertainties associated with the instrumentation readings. Even though the error associated with the thermocouple temperatures was 1°C as reported by Omega Engineering, we found a larger discrepancy between the readings at higher temperatures.

Table 3: Uncertainties associated with instrumentation readings

Instrumentation	**Error**
Type T Thermocouple	+/- 2.5 °C
Coriolis Flowmeter	1% of reading

4. RESULTS AND DISCUSSION FROM STEP RESPONSE TESTS

The experimentally derived Nusselt number is plotted as a function of time. The predicted Nusselt number is also plotted for the corresponding experimental runs. The predicted Nusselt number was calculated at each time step using the measured Reynolds and Prandtl numbers. The range of Reynolds and Prandtl numbers are given for each run in Table 2. The error bars from instrumentation readings and fluid property uncertainties have also been plotted. The results from control volume section 1 and 5, the entrance and exit sections respectively, are reported here. The temperature transient for Run 2 is also plotted as an example in Figure 7. Towards the end of the transient the temperature difference between the pebbles and the oil decreases, and thus the calculated heat transfer coefficient becomes arbitrarily large. Therefore these time steps are not taken into account in the calculation of the heat transfer coefficient.

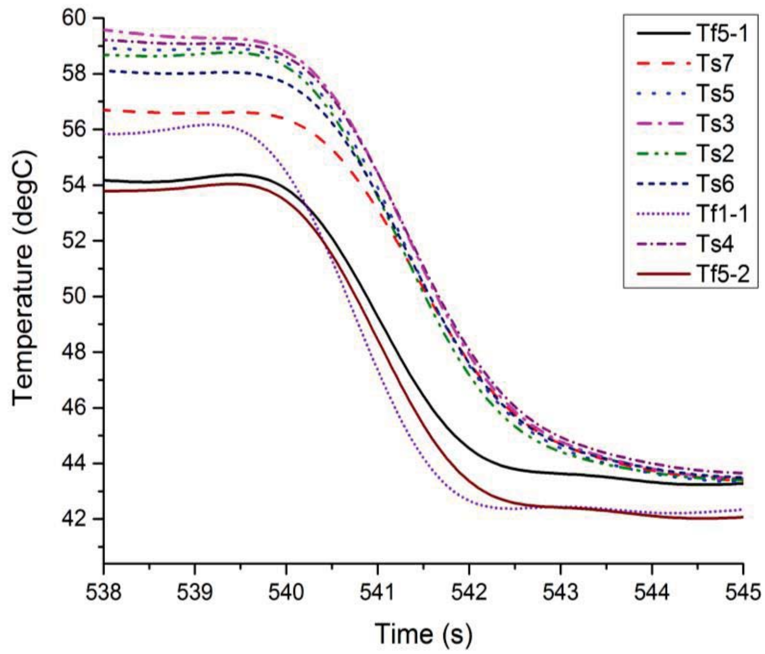

Figure 6: Smoothed therocouple readings as a function of time. Tf5-1, Tf5-2 and Tf1-1 are the fluid temperatures, and the rest are pebble temperatures

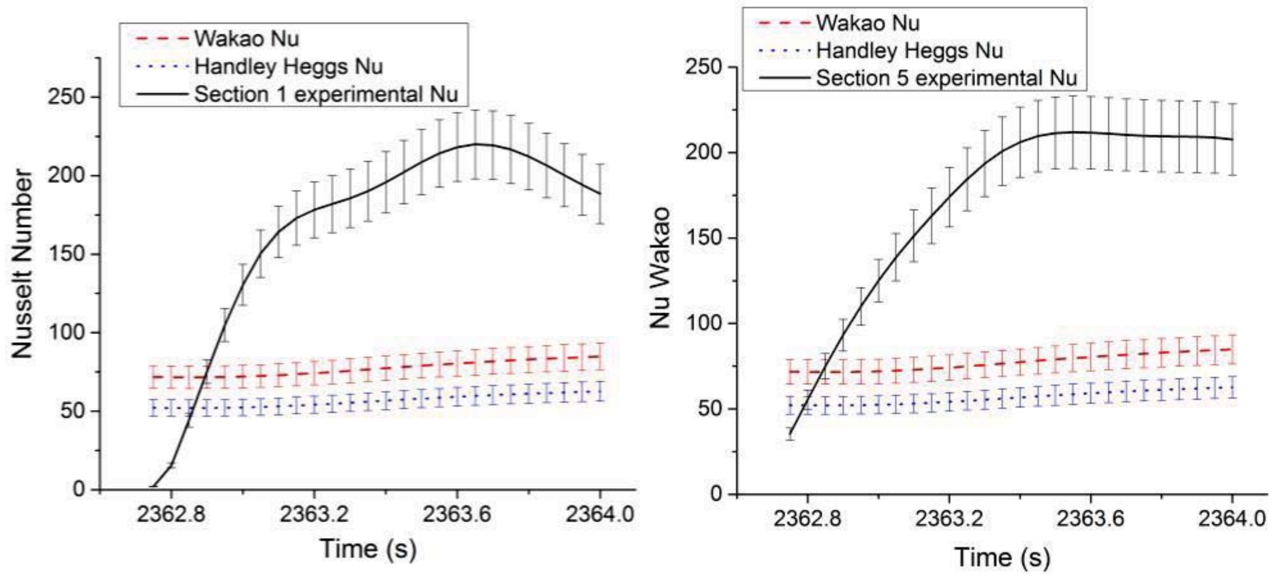

Figure 8: Nusselt number comparisons for Run 1

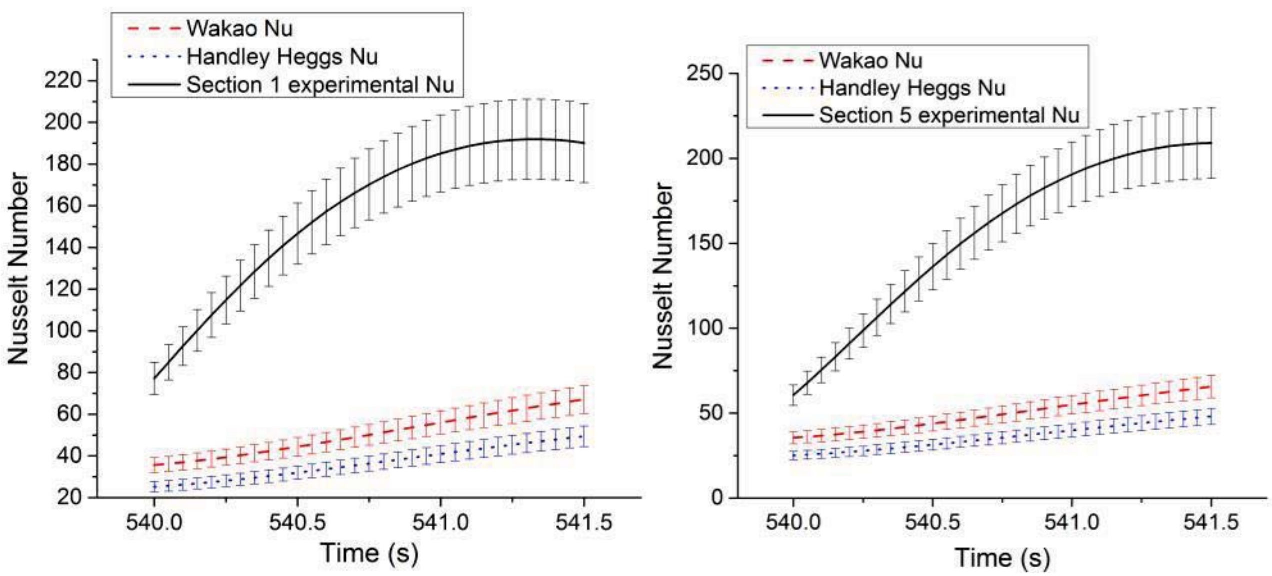

Figure 9: Nusselt number comparisons for Run 2

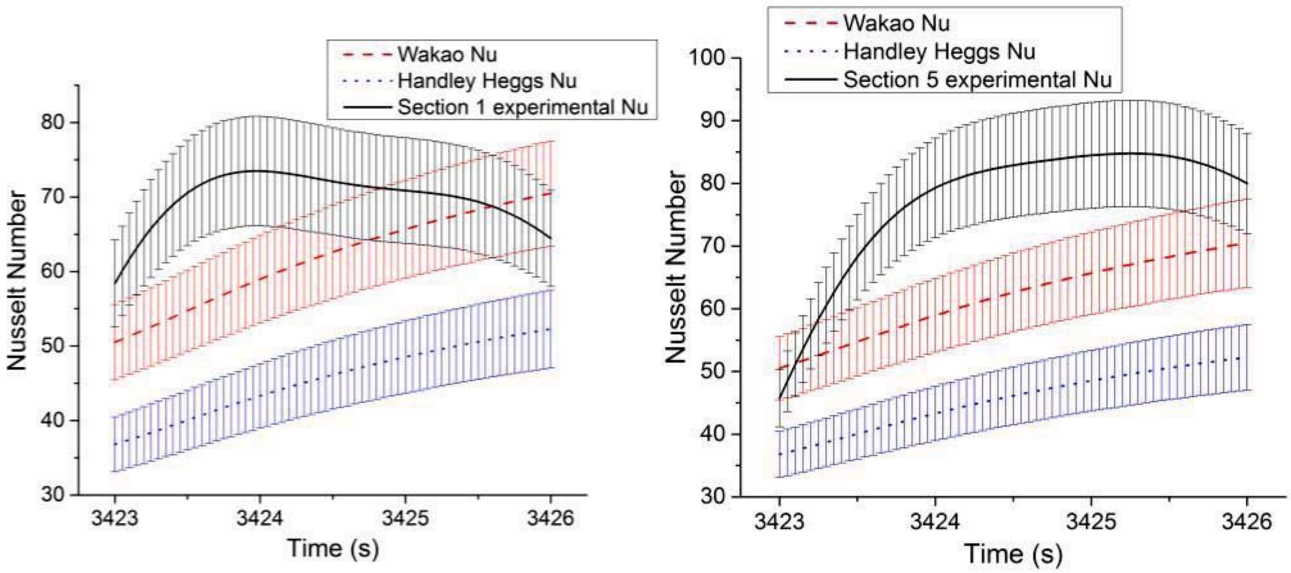

Figure 10: Nusselt number comparisons for Run 3

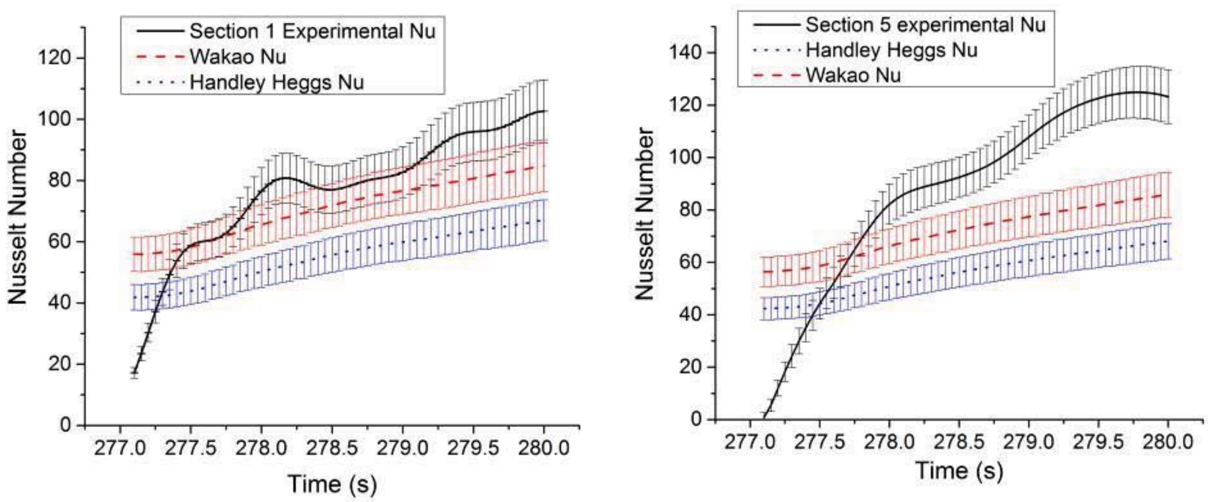

Figure 11: Nusselt number comparisons for Run 4

Figures 8 to 11 show the Nusselt numbers as a function of time for the entrance and exit control volume sections. During these runs the achieved Reynolds and Prandtl numbers were lower than the operating PB-FHR conditions, and this is partly because of the high viscosity of the Drakesol 260AT. In future iterations of this experiment, it would be better to use Dowtherm A as the operating fluid given that Prandtl numbers of 15 can be reached at a temperature of about 90 ˚C. Generally, it was found that the experimental Nusselt numbers were higher than the predicted correlations by up to 360 %. More experimental data for a lower Prandtl number and higher Reynolds number needs to be collected in order to draw any final conclusions. This is especially the case because a high temperature difference between the pebbles and the oil was not achieved.

5. EXPERIMENTAL DESIGN USING FREQUENCY RESPONSE TECHNIQUES

The data collected in the experimental facility described in Section 2 of this paper has significant uncertainty attached to it, and therefore the quality of the results can be substantially improved using other experimental techniques. For this reasons we are constructing a new experimental facility that will have the capability to perform tests that study the response of the test section temperature due to step changes in the fluid temperature (as before) and also due to sinusoidal changes in the fluid temperature. Frequency response techniques have been used previously to measure heat transfer coefficients in fluidized beds, in which the solid particles have an associated velocity [9]. One of the advantages of frequency response techniques outlined in these studies is that the solid temperature within the test section need not be directly measured. These studies use a model to estimate the solid and fluid temperatures within the test section. In UCB's test section, the temperatures of some of the copper spheres are measured. Thus we will have less uncertainty in the derived heat transfer coefficient compared to previous studies.

There are three main reasons we consider using frequency response techniques to measure heat transfer coefficients in the pebble-bed test section:

(1) In the data reduction procedure outlined in Section 3.1 of this paper, h is a function of the derivative of the pebble temperature T_s. With a step change in the pebble temperatures, the slope very steep and is thus subject to errors. If the pebble temperature was made to vary sinusoidally, the derivative could be easily obtained, and to a higher accuracy.
(2) The data collection period can be much longer than it was in the previous experiment as we would be operating the experiment under periodic steady state conditions, thereby reducing any potential distortions due to transient effects.
(3) With the new experimental configuration we would have more control over the minimum and maximum temperatures of the fluid, and thus we could have larger ΔT than was previously obtained. Thus more data can be collected.

5.1 Governing Equations in the Test Section and Analytical Solutions

The governing equations for the solid and fluid phases are given in Equations (11) and (12). The boundary conditions are also given (Equations (13) – (15)). These equations can be non-dimensionalized using the parameters in Equations (16) – (22). The non-dimensional governing equations and boundary conditions are given in Equations (23) – (27).These equations can be solved and used to predict the fluid and solid temperatures in the test section as a function of time and one spatial derivative. In the pre-prediction models, h will be estimated from the Wakao correlation [2].

$$\frac{\partial T_f}{\partial t} + v_z \frac{\partial T_f}{\partial z} = \frac{h_{sf}}{\varepsilon(\rho c_p)_f}(T_s - T_f) \tag{11}$$

$$\frac{\partial T_s}{\partial t} = \frac{h_{sf}}{(1-\varepsilon)(\rho c_p)_s}(T_f - T_s) \tag{12}$$

$$T_f(t=0) = T_{f0} \tag{13}$$

$$T_s(t=0) = T_{s0} = T_{f0} \tag{14}$$

$$T_f(z=0) = T_{f0} + \alpha T_{f0}\sin(\omega t) \tag{15}$$

In equations (11) to (15), T_{f0} is the initial fluid temperature in °C, T_{s0} the initial solid temperature in °C, α the amplitude of the fluid temperature oscillation and ω the frequency of the oscillation in s^{-1}.

$$F = \frac{T_f - T_{f0}}{\alpha T_{f0}} \tag{16}$$

$$S = \frac{T_s - T_{f0}}{\alpha T_{f0}} \tag{17}$$

$$x = \frac{z}{L} \tag{18}$$

$$\tau = \frac{h_{sf}}{(\rho c_p)_s} t \tag{19}$$

$$\phi = \frac{h_{sf} L}{\varepsilon v_z (\rho c_p)_f} \tag{20}$$

$$\sigma = \frac{h_{sf} L}{v_z (\rho c_p)_s} \tag{21}$$

$$\eta = \omega \frac{(\rho c_p)_s}{h_{sf}} \tag{22}$$

$$\sigma \frac{\partial F}{\partial \tau} + \frac{\partial F}{\partial x} = \phi(S - F) \tag{23}$$

$$\frac{\partial S}{\partial \tau} = \pi(F - S) \tag{24}$$

$$F(\tau = 0) = 0 \tag{25}$$

$$S(\tau = 0) = 0 \tag{26}$$

$$F(x = 0) = \sin(\eta \tau) \tag{27}$$

Here, π replaces $\frac{1}{(1-\varepsilon)}$ to simplify the equations.

Analytical solutions for the entrance section (section 1), where x = 0, can be determined and are given in Equations (27) and (28).

$$S(x = 0) = \frac{\pi^2 \sin \eta\tau - \pi\eta \cos \eta\tau}{\pi^2 + \eta^2} + \frac{\pi\eta e^{-\pi\tau}}{\pi^2 + \eta^2} \tag{28}$$

The solid and fluid non-dimensional temperatures as a function of non-dimensional time are shown in Figure 12. The solid temperature lags behind the fluid temperature, and this lag can be controlled by choosing the appropriate non-dimensional constants.

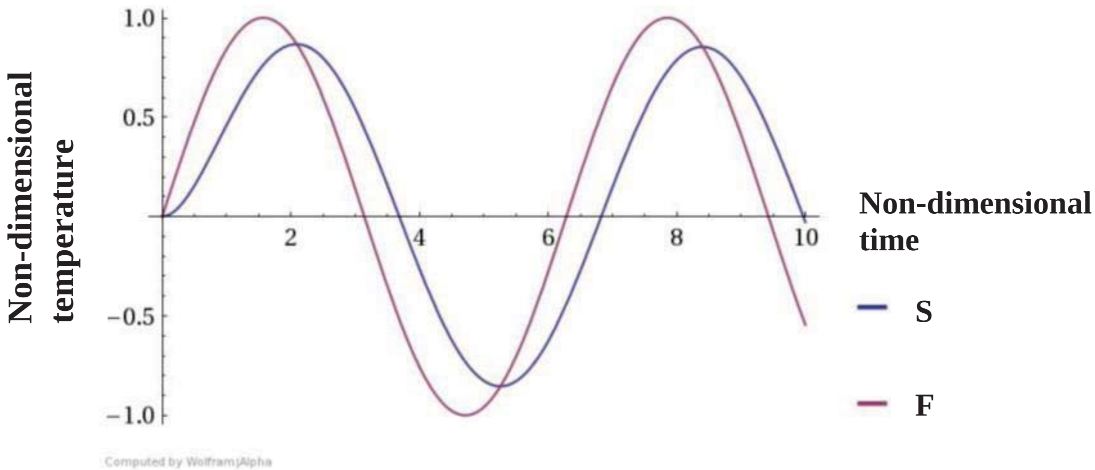

Figure 12: Fluid and solid non-dimensional temperatures as a function of time at the entrance (x = 0). The red line represents the fluid inlet temperature and the blue line represents the solid temperature

An appropriate frequency of the inlet fluid temperature needs to be determined. We can use the solutions at x = 0 to estimate an appropriate value for η, and thus ω. In order to do this, σ and φ do not need to be estimated, as they do not appear in the x = 0 solutions. The values for η and ε were used to plot the graph in Figure 12, where π was taken as 1.67 and η arbitrarily chosen as 1. The value of η can be adjusted depending on how much lag between the fluid and solid temperature is needed. It is important to note that during the experimental run, the numerical value of the non-dimensional numbers in equations (16) to (22) will change if they are dependent on h_{sf} or fluid properties. These are a function of temperature, and thus will be changing throughout the run.

5.2 Experimental Design

A schematic of the new experimental loop is shown in Figure 13. The operating fluid will be Dowtherm A in order to match the Prandtl number of flibe at lower temperatures than for Drakesol 260AT. The old thermocouples that were previously installed on the test section will be replaced with new and calibrated type T thermocouples. A tankless heater will be used to heat the oil. This type of heater was chosen for its low thermal inertia. It is designed to instantaneously heat water to the required temperature. The power into the heater will be controlled using a DC power supply. LabView will be used to control the DC power supply to the heater to allow for a sinusoidal heater power input. A plate-and-frame heat exchanger will be used to cool the fluid before it enters a large reservoir of the oil. There are no experimental constraints on choosing the frequency of the temperature oscillation, and thus it can be chosen freely. A variable speed drive controls the pump speed, thus allowing for easier control of the mass flow rate through the loop compared to the previous experiment.

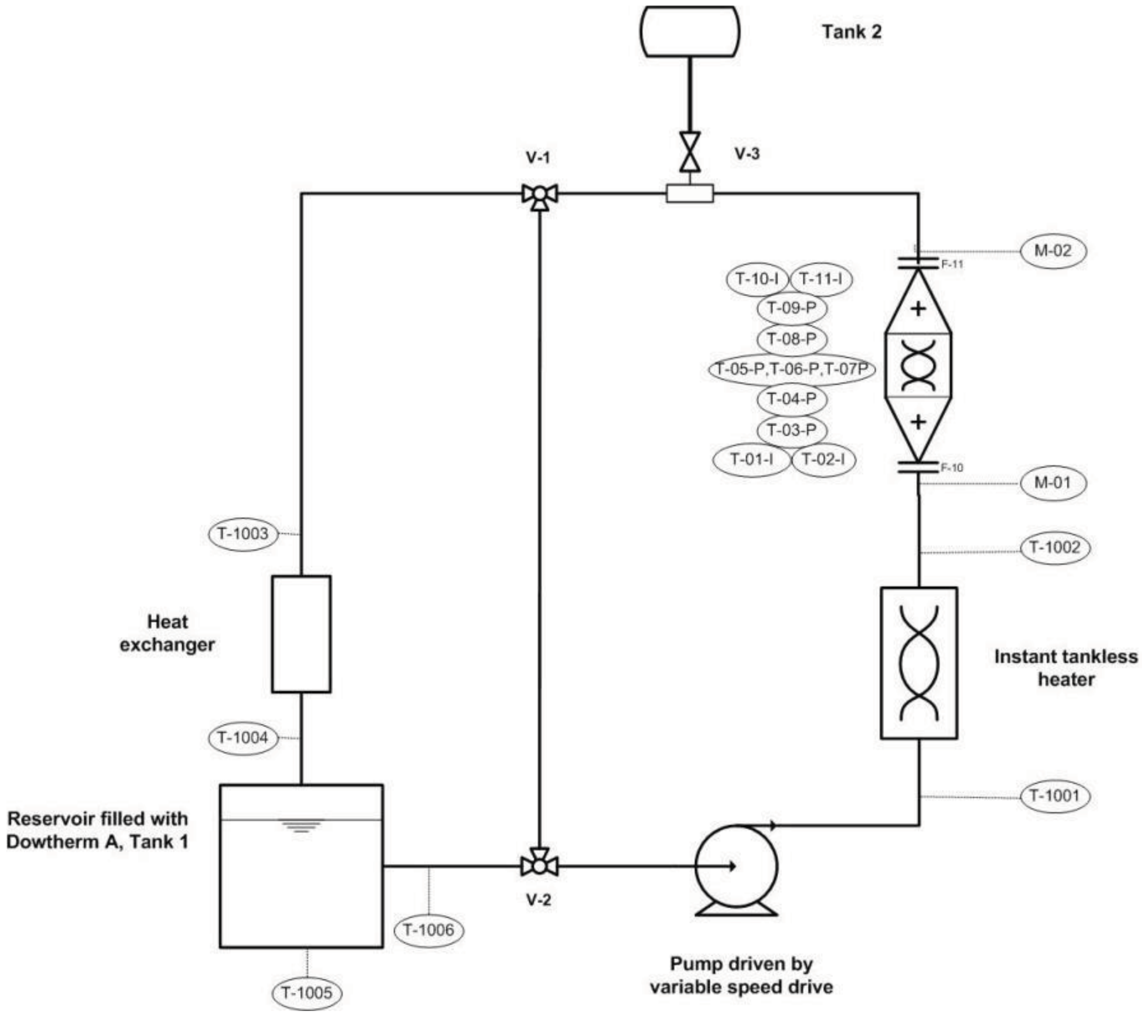

Figure 13: Diagram of the new experimental design including important components

6. CONCLUSIONS AND FUTURE WORK

The main aims of this investigation were to measure heat transfer coefficients in pebble beds and compare the measurements with predictive correlations. This was done in support of developing a better understanding of heat transfer in the PB-FHR reactor core. A test section filled with randomly packed copper spheres was heated to a certain temperature, after which a step change in the inlet fluid temperature was established. The temperatures of the fluid inlet and outlet were recorded throughout the transient, as well as the pebble temperatures. Experimental heat transfer coefficients were extracted from this. It was found that the correlations underestimated the experimental values. This needs further investigation, and the design of another experiment to study heat transfer coefficients using frequency response techniques was proposed.

7. ACKNOWLEDGEMENTS

This material is based upon work supported by the National Science Foundation Graduate Research Fellowship under Grant No DGE 1106400 and supported by the US Department of Energy Office of Nuclear Energy University Programs Integrated Research Project.

8. REFERENCES

[1] P. M. Bardet and P. F. Peterson, "Options for Scaled Experiments for High Temperature Liquid Salt and Helium Fluid Mechanics and Convective Heat Transfer," *Nucl. Technol.*, vol. 163, pp. 344–357, 2008.

[2] T. Wakao, N., Funazkri, "EFFECT OF FLUID DISPERSION COEFFICIENTS PARTICLE-TO-FLUID HEAT TRANSFER COEFFICIENTS IN PACKED BEDS," *Chem. Eng. Sci.*, 1979.

[3] L. P. Carillo, "Convective heat transfer for viscous fluid flow through a metallic packed bed," *Interciencia*, vol. 30, no. 2, p. 81, 2005.

[4] D. Geb and I. Catton, "Internal Heat Transfer Coefficient Determination in a Packed Bed From the Transient Response Due to Solid Phase Induction Heating," vol. 134, no. April, 2012.

[5] P. J. Handley, D., Heggs, "Momentum and Heat Transfer Mechanisms in Regular Shaped Packings," *Trans. Inst. Chem. Eng.*, vol. 46, no. 9, 1968.

[6] P. F. Andreades, C., Cisneros, A. T., Choi, J. K., Chong, A. Y. K., Fratoni, M., Hong, S., Huddar, L., Huff, K. D., Krumweide, D. L., Laufer, M. R., Munk, M., Scarlat, R. O., Zweibaum, N., Greenspan, E., Peterson, "Technical Description of the 'Mark 1' Pebble-Bed Fluoride-Salt-Cooled High Temperature Reactor (PB-FHR) Power Plant," 2014.

[7] N. S. S. C. (KTA), "Nuclear Safety Standards Commission (KTA) Reactor Core Design of High-Temperature Gas-Cooled Reactors Part 2 : Heat Transfer in Spherical Fuel Elements (June 1983)," 1983.

[8] D. L. Dixon, A. G., Cresswell, "Theoretical Prediction of Effective Heat Transfer Parameters in Packed Beds," *AIChE J.*, vol. 25, no. 4, pp. 663–676, 1979.

[9] A. P. Littman, H., Stone, "Gas-Particle Heat Transfer Coefficients in Fluidized Beds by Frequency Response Techniques," *Fluid Part. Technol. - Chem. Eng. Prog. Symp. Ser.*, vol. 62, 1966.